Inter-Vector Interference Self-Cancellation Scheme for Differential OSDM in Underwater Acoustic Communications

Wang, Yujie; Zhang, Qunfei; Ma, Shengqian; Zhang, Lingling; Han, Jing; Leus, Geert

DOI
10.1109/SPAWC53906.2023.10304441

Publication date
2023

Document Version
Final published version

Published in
Proceedings of the 2023 IEEE 24th International Workshop on Signal Processing Advances in Wireless Communications (SPAWC)

Citation (APA)
Wang, Y., Zhang, Q., Ma, S., Zhang, L., Han, J., & Leus, G. (2023). Inter-Vector Interference Self-Cancellation Scheme for Differential OSDM in Underwater Acoustic Communications. In *Proceedings of the 2023 IEEE 24th International Workshop on Signal Processing Advances in Wireless Communications (SPAWC)* (pp. 501-505). IEEE. https://doi.org/10.1109/SPAWC53906.2023.10304441

2023 IEEE 24th International Workshop on Signal Processing Advances in Wireless Communications (SPAWC) | 978-1-6654-9626-1/23/$31.00 ©2023 IEEE | DOI: 10.1109/SPAWC53906.2023.10304441

Inter-Vector Interference Self-Cancellation Scheme for Differential OSDM in Underwater Acoustic Communications

Yujie Wang[1], Qunfei Zhang[1], Shengqian Ma[1], Lingling Zhang[1], Jing Han[1], and Geert Leus[2]
[1] *School of Marine Science and Technology, Northwestern Polytechnical University, Xi'an 710072, China*
[2] *Faculty of Electrical Engineering, Mathematics and Computer Science, Delft University of Technology, Delft 2826 CD, The Netherlands*

***Abstract*—Differential orthogonal signal-division multiplexing (OSDM) is attractive for underwater acoustic (UWA) communications because it can eliminate channel estimation, resulting in a substantial reduction of complexity at the receiver. However, when the channel is time-varying, it may suffer from serious inter-vector interference (IVI), which is similar to inter-carrier interference (ICI) in differential orthogonal frequency-division multiplexing (OFDM). To mitigate this degradation of system performance, this paper provides a novel two-hop differential OSDM system based on IVI self-cancellation. Although this method improves system reliability at the cost of losing data rate, it is easy to implement in UWA modems. Finally, numerical simulations demonstrate the effectiveness of the proposed two-hop differential OSDM system over time-varying UWA channels.**

***Index Terms*—Differential OSDM, IVI self-cancellation, time-varying channels, underwater acoustic communications.**

I. Introduction

Up to now, underwater acoustic communication (UWA) is still the first choice for oceanographic data collection and transmission [1]. However, limited by UWA channels, establishing a high-speed and robust UWA communication system has its unique difficulties [2]. To be specific, the large propagation loss of the UWA channels and the obvious frequency dependence of channel absorption limit the bandwidth of UWA communication systems, usually below the order of 10 kHz, which has a notable impact on the transmission data rate [3]. Furthermore, boundary reflection and medium scattering in UWA channel transmission result in a significant multipath spread of UWA communication signals, usually on the order of 10 ms to 100 ms, which seriously affects the link reliability [3], [4]. In addition, platform motion can produce extreme Doppler effects, with corresponding Doppler factors typically in the range of 10^{-3} to 10^{-4}, which is about five orders of magnitude higher than for wireless radio channels [4], [5]. This will also seriously influence the reliability of the UWA communication system.

To overcome channel fading and achieve high-rate transmission, orthogonal frequency-division multiplexing (OFDM) and single-carrier frequency-domain equalization (SC-FDE) are two popular UWA communication schemes. Specifically, the attractiveness of OFDM lies in its ability to convert a frequency-selective channel into a set of parallel frequency-flat subchannels, allowing for efficient elimination of inter-symbol interference (ISI) through one-tap equalization on each subcarrier [6]. However, due to the superposition of data symbols on a large number of subcarriers, OFDM systems encounter a significant peak-to-average power ratio (PAPR) [7]. In contrast, SC-FDE can achieve lower PAPR through applying the discrete Fourier transform (DFT) and inverse DFT (IDFT) operations at the receiver, but its bandwidth management and power allocation are not flexible enough [8], [9].

In recent years, a generalized modulation named orthogonal signal-division multiplexing (OSDM) has gradually received widespread attention [10], [11]. OSDM introduces the concept of "symbol vector" and unifies OFDM and SC-FDE as two extreme implementations under this framework, thereby achieving the integration of multi-carrier and single-carrier modulation schemes [15]. In particular, OSDM divides the data block into several symbol vectors and performs component-wise IDFTs with a reduced length equal to the number of vectors. By adjusting the length of symbol vectors, the OSDM system can achieve lower PAPR (compared to OFDM) and more flexible bandwidth management (compared to SC-FDE).

However, so far most efforts on OSDM UWA communication require channel estimation at the receiver [12]–[15], which may lead to high computational complexity, especially in the high-frequency band and high-rate scenarios. This motivates us to resort to differential detection as an alternative, since it does not need channel estimation [16]. Also, unlike the conventional scheme where the differential encoding is performed between adjacent blocks, in this paper the differential OSDM scheme is based on adjacent symbol vectors. The aim of this design is to relax the assumption that the channel is fixed over consecutive blocks. However, this could still be not enough for some UWA channels where the time variations within one block is non-negligible. In this case, the Doppler spread destroys the orthogonality of the vectors leading to inter-vector interference (IVI). This is similar to inter-carrier interference (ICI) in OFDM

This work was supported by National Natural Science Foundation of China under Grants 62171384 and 62271397. The work of Y. Wang was supported by the China Scholarship Council. (Corresponding author: Jing Han, electronic mail: hanj@nwpu.edu.cn.)

and significantly degrades the system performance [14]. To solve the problem, a two-hop differential OSDM system is further proposed to achieve IVI self-cancellation. The main contributions of this paper are summarized as follows.

1) *Signal Model*: The signal model of differential OSDM is derived, from which it is shown that the symbol vectors can be decoupled at the receiver over frequency-selective fading channels. Since each element in the symbol vector can be regarded as a transmit antenna, we can adopt the differential unitary space-time modulation (USTM) from [17] and [18] to design the information transfer matrix. This will allow us to capture the multipath diversity.

2) *Interference Cancellation*: An IVI self-cancellation method is designed, which can be deemed as an analog of the ICI self-cancellation method [19]. The main idea is to modulate data symbols onto adjacent symbol vectors with predefined weighting coefficients. Based on this, a two-hop differential encoding scheme is designed to upgrade the differential OSDM system. Although this method sacrifices data rate, it is easy to implement and can improve the reliability of the differential OSDM over time-varying channels.

The remainder of this paper is organized as follows. In Section II, we present the differential OSDM signal model over time-invariant and time-varying channels. Based on that, in Section III, we propose a self-cancellation method to address the impact of IVI on the differential OSDM system. Numerical simulation results are then presented in Section IV. Finally, conclusions are drawn in Section V.

The notation used in this paper is summarized as follows. Bold upper (lower) letters denote matrices (column vectors); $(\cdot)^*$, $(\cdot)^T$, and $(\cdot)^H$ stand for conjugate, transpose, and Hermitian transpose. We reserve $\otimes$ for the Kronecker product, $\|\cdot\|$ for the Frobenius norm, and $(\cdot)_K$ for the modulo-K operation. We use $\mathbf{I}_N$ and $\mathbf{e}_N(n)$ to represent the $N \times N$ identity matrix and its nth column, respectively. Also, we define $[\mathbf{x}]_n$ as the nth entry of the vector $\mathbf{x}$, and $[\mathbf{X}]_{m,n}$ as the (m,n)th entry of the matrix $\mathbf{X}$, where all indices are starting from 0. Similarly, $[\mathbf{x}]_{m:n}$ indicates the subvector of $\mathbf{x}$ from entry m to n, and $[\mathbf{X}]_{m:n,p:q}$ indicates the submatrix of $\mathbf{X}$ from row m to n and from column p to q. Moreover, we use $\mathrm{diag}\{\mathbf{x}\}$ to represent a diagonal matrix with $\mathbf{x}$ on its diagonal. In addition, $\mathbf{F}_N$ refers to the $N \times N$ unitary DFT matrix, i.e., $[\mathbf{F}_N]_{p,q} = N^{-1/2} e^{-j2\pi pq/N}$.

II. Signal Model

In this section, we present the signal model of the differential OSDM system. For simplicity, we first build the signal model for time-invariant channels. Then, based on this, we introduce Doppler spread and establish the differential OSDM signal model over time-varying channels.

A. Signal Model for Time-Invariant Channels

Let us consider a differential OSDM block with $K = MN$ differentially encoded symbols denoted by $\mathbf{d} = [d_0, d_1, \ldots, d_{K-1}]^T$. The transmitted block $\mathbf{d}$ is partitioned into N symbol vectors of length M, i.e.,

$$\mathbf{d}_n = [d_{nM}, d_{nM+1}, \ldots, d_{nM+M-1}]^T, \tag{1}$$

for $n = 0, \ldots, N-1$. Subsequently, each symbol vector is written row-wise into an $N \times M$ matrix. Then, M component-wise N-point IDFTs are implemented, and the entries of the resulting matrix are read out row-wise to obtain the length-K transmitted signal. This whole process can be formulated as

$$\begin{aligned} \mathbf{s} &= \mathbf{P}_{N,M}^H (\mathbf{I}_M \otimes \mathbf{F}_N^H) \mathbf{P}_{N,M} \mathbf{d} \\ &= (\mathbf{F}_N^H \otimes \mathbf{I}_M) \mathbf{d}, \end{aligned} \tag{2}$$

where $\mathbf{P}_{N,M}$ is the $K \times K$ permutation matrix defined as

$$\mathbf{P}_{N,M} = \begin{bmatrix} \mathbf{I}_N \otimes \mathbf{e}_M^T(0) \\ \mathbf{I}_N \otimes \mathbf{e}_M^T(1) \\ \vdots \\ \mathbf{I}_N \otimes \mathbf{e}_M^T(M-1) \end{bmatrix}. \tag{3}$$

Finally, a cyclic prefix (CP) is added to the differential OSDM transmission block $\mathbf{s}$ as the protection interval.

At the receiver, the baseband received signal after CP removal can be expressed as

$$\mathbf{r} = \widetilde{\mathbf{H}} \mathbf{s} + \mathbf{n} \tag{4}$$

where $\widetilde{\mathbf{H}}$ is the $K \times K$ circulant channel matrix, with the first column equal to the time-invariant channel impulse response (CIR) vector $\mathbf{h} = [h_0, h_1, \ldots, h_L]^T$ appended by $K - L - 1$ zeros and where $\mathbf{n}$ is the additive noise term. Then, by performing M component-wise N-point DFTs, we obtain

$$\begin{aligned} \mathbf{x} &= \mathbf{P}_{N,M}^H (\mathbf{I}_M \otimes \mathbf{F}_N) \mathbf{P}_{N,M} \mathbf{r} \\ &= (\mathbf{F}_N \otimes \mathbf{I}_M) \mathbf{r}. \end{aligned} \tag{5}$$

Based on (4), the demodulated block can be rewritten as

$$\begin{aligned} \mathbf{x} &= (\mathbf{F}_N \otimes \mathbf{I}_M)\, \mathbf{r} \\ &= \mathbf{C}\mathbf{d} + \mathbf{z} \end{aligned} \tag{6}$$

where

$$\mathbf{C} = (\mathbf{F}_N \otimes \mathbf{I}_M)\, \widetilde{\mathbf{H}} \left(\mathbf{F}_N^H \otimes \mathbf{I}_M \right) \tag{7}$$

is the $K \times K$ composite channel matrix and $\mathbf{z}$ is the $K \times 1$ demodulated noise term.

By utilizing the property that the circulant channel matrix can be diagonalized by the DFT matrix, the circulant channel matrix $\widetilde{\mathbf{H}}$ can be decomposed as

$$\begin{aligned} \widetilde{\mathbf{H}} &= \mathbf{F}_K^H \mathrm{diag}\{[H_0, H_1, \ldots, H_{K-1}]\}\, \mathbf{F}_K \\ &= \mathbf{F}_K^H \mathbf{P}_{N,M} \bar{\mathbf{H}} \mathbf{P}_{N,M}^H \mathbf{F}_K, \end{aligned} \tag{8}$$

where

$$\bar{\mathbf{H}} = \begin{bmatrix} \bar{\mathbf{H}}_0 & & & \\ & \bar{\mathbf{H}}_1 & & \\ & & \ddots & \\ & & & \bar{\mathbf{H}}_{N-1} \end{bmatrix} \tag{9}$$

with $\bar{\mathbf{H}}_n = \mathrm{diag}\{[H_n, H_{N+n}, \ldots, H_{(M-1)N+n}]^T\}$ as the decimated frequency response submatrix, since $H_k = \sum_{l=0}^{L} h_l e^{-j(2\pi/K)lk}$ for $k = 0, 1, \ldots, K-1$.

Let us now introduce a proposition on the decomposition of the DFT unitary matrix [15]: If $K = M \times N$, then the $K \times K$ DFT matrix $\mathbf{F}_K$ can be factorized as

$$\mathbf{F}_K = \mathbf{P}_{N,M}(\mathbf{I}_N \otimes \mathbf{F}_M)\mathbf{\Lambda}(\mathbf{F}_N \otimes \mathbf{I}_M) \tag{10}$$

where

$$\mathbf{\Lambda} = \begin{bmatrix} \mathbf{\Lambda}_M^0 & & & \\ & \mathbf{\Lambda}_M^1 & & \\ & & \ddots & \\ & & & \mathbf{\Lambda}_M^{N-1} \end{bmatrix} \tag{11}$$

with $\mathbf{\Lambda}_M^n = \mathrm{diag}\{[1, e^{-j\frac{2\pi n}{K}}, \ldots, e^{-j\frac{2\pi n}{K}(M-1)}]^T\}$ for $n = 0, 1, \ldots, N-1$. Further, substituting (10) into (8), we find that the composite channel matrix $\mathbf{C}$ has a block diagonal structure, i.e.,

$$\mathbf{C} = \begin{bmatrix} \mathbf{H}_0 & & & \\ & \mathbf{H}_1 & & \\ & & \ddots & \\ & & & \mathbf{H}_{N-1} \end{bmatrix} \tag{12}$$

where

$$\mathbf{H}_n = \mathbf{\Lambda}_M^{nH}\mathbf{F}_M^H\bar{\mathbf{H}}_n\mathbf{F}_M\mathbf{\Lambda}_M^n. \tag{13}$$

Thus, the N differentially encoded symbol vectors can be separated at the receiver as

$$\mathbf{x}_n = \mathbf{H}_n\mathbf{d}_n + \mathbf{z}_n, \quad n = 0, \ldots, N-1. \tag{14}$$

Here, using (13) to expand (14), we have

$$\mathbf{x}_n = \mathbf{\Lambda}_M^{nH}\mathbf{F}_M^H\bar{\mathbf{H}}_n\mathbf{F}_M\mathbf{\Lambda}_M^n\mathbf{d}_n + \mathbf{z}_n. \tag{15}$$

Moreover, defining $\bar{\mathbf{x}}_n = \mathbf{F}_M\mathbf{\Lambda}_M^n\mathbf{x}_n$, $\bar{\mathbf{d}}_n = \mathbf{F}_M\mathbf{\Lambda}_M^n\mathbf{d}_n$, and $\bar{\mathbf{z}}_n = \mathbf{F}_M\mathbf{\Lambda}_M^n\mathbf{z}_n$, the output of the differential OSDM system can be presented as

$$\bar{\mathbf{x}}_n = \bar{\mathbf{H}}_n\bar{\mathbf{d}}_n + \bar{\mathbf{z}}_n. \tag{16}$$

Let us now explain how the data is differentially encoded and decoded. By defining $\mathcal{B}$ as a finite group of $M \times M$ unitary and diagonal matrices, the generation of $\bar{\mathbf{d}}_n$ follows the recursion

$$\bar{\mathbf{d}}_n = \begin{cases} \mathbf{B}_n\bar{\mathbf{d}}_{n-1}, & 1 \le n \le N-1 \\ \mathbf{I}_M, & n = 0 \end{cases} \tag{17}$$

where $\mathbf{B}_n \in \mathcal{B}$ is the information transfer matrix corresponding to the nth symbol vector. The work [21] has proven that the maximum multipath diversity and high coding advantages can be obtained by using the USTM constellation group designed in [17]. So this paper will not focus on the design of the information transfer matrix group, and we will directly use the results given in [17].

Under the assumption that the channel does not change much over two consecutive symbol vectors, i.e., $\bar{\mathbf{H}}_n \approx \bar{\mathbf{H}}_{n-1}$, we can obtain from (16) that

$$\bar{\mathbf{x}}_n = \mathbf{B}_n\bar{\mathbf{x}}_{n-1} + \bar{\mathbf{w}}_n, \tag{18}$$

where $\bar{\mathbf{w}}_n = \bar{\mathbf{z}}_n - \mathbf{B}_n\bar{\mathbf{z}}_{n-1}$ is the differential noise term. Based on (18), the maximum-likelihood (ML) detector of the differential OSDM system can be represented by

$$\widehat{\mathbf{B}}_n = \arg\min_{\mathbf{B}\in\mathcal{B}} \|\bar{\mathbf{x}}_n - \mathbf{B}\bar{\mathbf{x}}_{n-1}\|^2. \tag{19}$$

And the complexity of the ML receiver is exponentially related to the vector length M.

B. Signal Model for Time-Varying Channels

In UWA communications, we often deal with time-varying channels. In this case, (4) can still describe the input-output relationship of the channel. But the time-domain channel matrix $\widetilde{\mathbf{H}}$ no longer has a circulant structure, since it has entries

$$[\widetilde{\mathbf{H}}]_{k,k'} = h_{k,(k-k')_K}, \quad 0 \le k, k' \le K-1, \tag{20}$$

where $h_{k,l}$ represents the time-varying CIR at the kth time instant and the lth delay tap. Also, the composite channel matrix $\mathbf{C}$ no longer has the block diagonal structure as in (12), and can now be expressed as [22]

$$\mathbf{C} = \left[\mathbf{\Lambda}^H\left(\mathbf{I}_N \otimes \mathbf{F}_M^H\right)\right]\bar{\mathbf{C}}\left[\left(\mathbf{I}_N \otimes \mathbf{F}_M\right)\mathbf{\Lambda}\right] \tag{21}$$

where $\bar{\mathbf{C}} = \mathbf{P}_{N,M}^{\mathrm{H}}\widehat{\mathbf{C}}\mathbf{P}_{N,M}$ and $\widehat{\mathbf{C}} = \mathbf{F}_K\widetilde{\mathbf{H}}\mathbf{F}_K^H$. As such, the matrix $\bar{\mathbf{C}}$ is a full matrix. By partitioning it into $M \times M$ blocks

$$\bar{\mathbf{C}}_{n,n'} = [\bar{\mathbf{C}}]_{nM:nM+M-1,n'M:n'M+M-1} \tag{22}$$

for $0 \le n, n' \le N-1$, and then inserting it into (6), we can write

$$\bar{\mathbf{x}}_n = \bar{\mathbf{C}}_{n,n}\bar{\mathbf{d}}_n + \sum_{n\neq n'}\bar{\mathbf{C}}_{n,n'}\bar{\mathbf{d}}_{n'} + \bar{\mathbf{z}}_n. \tag{23}$$

It can be seen that the second term on the right hand side represents the IVI, which is similar to the ICI in OFDM. This implies that the orthogonality among the N vectors in OSDM is destroyed when transmitted over time-varying channels. Therefore, we introduce IVI self-cancellation and propose a two-hop encoding scheme for the differential OSDM system in this paper, which will be described in Section III.

III. Inter-vector Interference Self-Cancellation

The IVI self-cancellation scheme in this paper is similar to the ICI self-cancellation scheme in [19]. It does not need channel estimation and only performs two simple steps to suppress IVI, which is suitable for the differential OSDM system and avoids the difficulties of the IVI equalization algorithms at the receiver [14], [15]. Specifically, the IVI self-cancellation scheme first modulates one set of data symbols onto a group of adjacent vectors with a group of weighting coefficients at the transmitter. The weighting coefficients are selected to minimize IVI caused by these vectors. Then, IVI self-cancellation demodulation is performed at the receiver by linearly combining adjacent symbol vectors with proposed coefficients to further reduce the residual IVI. Here we consider one of the simplest forms where two adjacent vectors are grouped and weighted by $(+1, -1)$, and a two-hop differential OSDM scheme is thus designed. Let us detail this next.

By assuming that the transmitted symbol vectors follow the relationship $\bar{\mathbf{d}}_1 = -\bar{\mathbf{d}}_0, \bar{\mathbf{d}}_3 = -\bar{\mathbf{d}}_2, \ldots, \bar{\mathbf{d}}_{N-1} = -\bar{\mathbf{d}}_{N-2}$, the nth received symbol vector becomes

$$\bar{\mathbf{x}}'_n = \sum_{\substack{n'=0 \\ n'=\text{even}}}^{N-2} \mathbf{V}'_{n,n'}\bar{\mathbf{d}}_{n'} + \bar{\mathbf{z}}_n \tag{24}$$

where $\mathbf{V}'_{n,n'} = \bar{\mathbf{C}}_{n,n'} - \bar{\mathbf{C}}_{n,n'+1}$ is the coefficient of IVI self-cancellation modulation. Further, the $(n+1)$th symbol vector is

$$\bar{\mathbf{x}}'_{n+1} = \sum_{\substack{n'=0 \\ n'=\text{even}}}^{N-2} \mathbf{V}'_{n+1,n'}\bar{\mathbf{d}}_{n'} + \bar{\mathbf{z}}_{n+1}. \tag{25}$$

It can be seen that only even numbers are taken for summation in (24) and (25), resulting in half the amount of interference signals compared to (23) for the conventional OSDM system. Thus, the IVI which affects the orthogonality of the symbol vectors will become smaller compared to (23). Then, the IVI self-cancellation demodulation is completed by subtracting adjacent received symbol vectors. In other words, we construct

$$\begin{aligned} \bar{\mathbf{x}}''_n &= \bar{\mathbf{x}}'_n - \bar{\mathbf{x}}'_{n+1} \\ &= \sum_{\substack{n'=0 \\ n'=\text{even}}}^{N-2} \mathbf{V}''_{n,n'}\bar{\mathbf{d}}_{n'} + \bar{\mathbf{z}}_n - \bar{\mathbf{z}}_{n+1} \end{aligned} \tag{26}$$

where $\mathbf{V}''_{n,n'} = \bar{\mathbf{C}}_{n,n'} + \bar{\mathbf{C}}_{n+1,n'+1} - \bar{\mathbf{C}}_{n+1,n'} - \bar{\mathbf{C}}_{n,n'+1}$ is the coefficient of IVI self-cancellation demodulation. Similar to the analysis method of ICI coefficients in [19], it is not difficult to observe that $\left\|\mathbf{V}''_{n,n'}\right\|$ is smaller than $\left\|\mathbf{V}'_{n,n'}\right\|$. Accordingly, at the receiver, IVI self-cancellation demodulation is further used to make the channel time-invariant. In this case, we can complete the subsequent processing through the differential method proposed in Section II. The only difference is that the differential operation here is no longer performed between adjacent symbol vectors, but between symbol vectors that are two hops away. And this two-hop differential scheme does not cause significant performance loss when the Doppler effect is not too severe.

More specifically, the output of the differential OSDM system after IVI cancellation can be represented as

$$\bar{\mathbf{x}}''_n = \mathbf{V}''_n\bar{\mathbf{d}}_n + \bar{\mathbf{z}}''_n \tag{27}$$

where n is assumed to be even, and $\mathbf{V}''_n$ and $\bar{\mathbf{z}}''_n$ are the channel matrix and noise term after IVI self-cancellation, respectively. Subsequently, the recursive representation of $\bar{\mathbf{d}}_n$ given by (17) will become

$$\bar{\mathbf{d}}_n = \begin{cases} \mathbf{B}_n\bar{\mathbf{d}}_{n-2}, & 1 < n < N-1 \\ \mathbf{I}_M, & n = 0 \end{cases}. \tag{28}$$

Afterwards, based on the assumption that the channel does not change much over two hops, i.e., $\mathbf{V}''_n \approx \mathbf{V}''_{n-2}$, we can obtain that

$$\bar{\mathbf{x}}''_n = \mathbf{B}_n\bar{\mathbf{x}}''_{n-2} + \tilde{\mathbf{z}}''_n \tag{29}$$

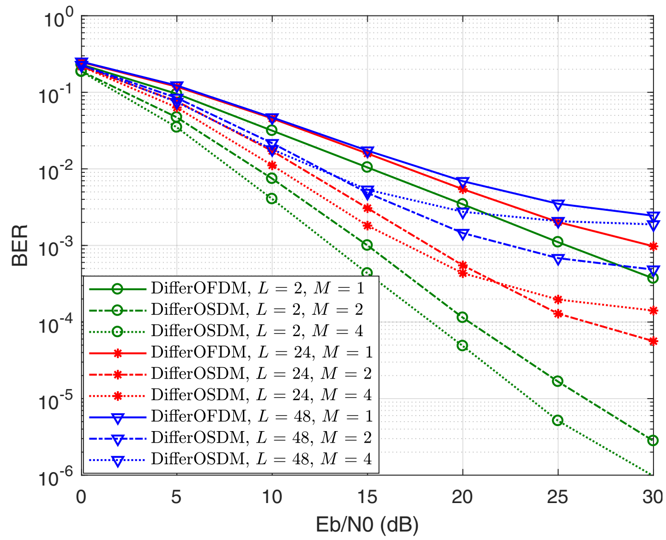

Fig. 1. BER performance of the proposed differential OSDM system over time-invariant channels with various channel memory lengths L.

where $\tilde{\mathbf{z}}''_n = \bar{\mathbf{z}}''_n - \mathbf{B}_n\bar{\mathbf{z}}''_{n-2}$ is the differential noise term. Finally, the ML detector in (19) can be rewritten as

$$\widehat{\mathbf{B}}_n = \arg\min_{\mathbf{B}\in\mathcal{B}} \left\|\bar{\mathbf{x}}''_n - \mathbf{B}_n\bar{\mathbf{x}}''_{n-2}\right\|^2. \tag{30}$$

IV. NUMERICAL SIMULATIONS

In this section, numerical simulation results are provided to evaluate the bit error rate (BER) performance of the proposed differential OSDM system. We consider the UWA communication scenario, where each differential OSDM block contains $K = 1024$ symbols and the block duration is $T = 20.48$ ms. So the symbol sampling period is $T_s = 0.02$ ms. Moreover, the channel taps are independent and identically distributed, zero-mean complex Gaussian variables with variance $\sigma_h^2 = 1/(L+1)$. With the above settings, the performance of the proposed system is illustrated in the following two parts.

1) *Effects of the Channel Multipath Spread*: Fig. 1 shows the BER performance of the proposed differential OSDM system over time-invariant channels with various channel memory lengths $L = 2$, 24, and 48. Here, we set three symbol vector lengths $M = 1, 2$, and 4, and when $M = 1$, differential OSDM is actually equivalent to differential OFDM. It can be seen that the proposed differential OSDM outperforms its OFDM counterpart, and the system can achieve a lower BER as M increases with short channel memory length $L = 2$. The reason for this is that a longer symbol vector length has the capacity to obtain more intra-vector frequency diversity gain [15]. And this diversity gain is indeed captured by the use of USTM [17]. However, as L increases, the assumption that the channel does not change much over two consecutive symbol vectors will no longer hold, and the differential OSDM system performance degrades accordingly. Meanwhile, the BER performance no longer decreases with the increase of M in the case of long channel memory length (i.e., $L = 24$), as the approximate frequency-domain channel equality gets less accurate when M

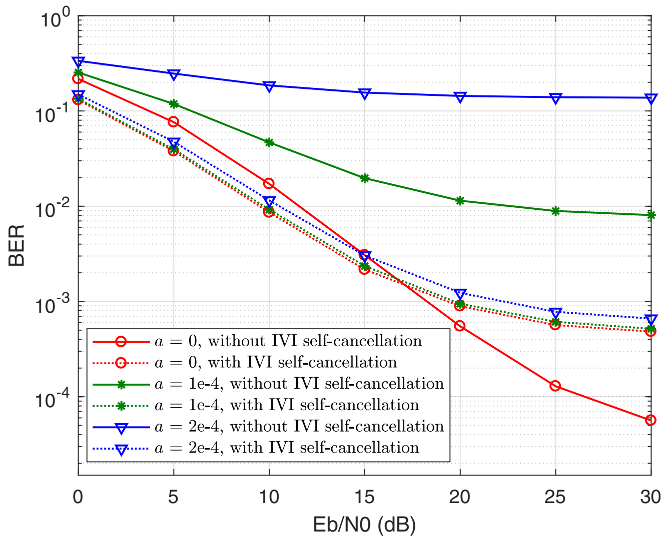

Fig. 2. BER performance of the proposed two-hop differential OSDM system with different Doppler scaling factors.

increases. A possible approach to alleviate this problem could be to use a multiband design as in [20] for OFDM systems. Although this topic warrants further investigation, it is beyond the scope of this paper.

2) *Impact of Channel Doppler Spread*: Fig. 2 illustrates the BER performance of the proposed two-hop differential OSDM system based on the IVI self-cancellation method. We here use different values of the Doppler scaling factor $a = 0$, 1×10^{-4} and 2×10^{-4} to introduce the channel Doppler effect. Meanwhile, the BER curves without IVI self-cancellation are also included as a benchmark. In addition, the symbol vector length and channel memory length are fixed to $M = 2$ and $L = 24$, respectively. It can be seen that the differential OSDM system can hardly work due to the lack of Doppler compensation. In contrast, by using the IVI self-cancellation method, the performance of the two-hop differential OSDM system can be considerably enhanced. Also, it should be noted that the crossing of the BER curves in the case of $a = 0$ is due to the different assumptions on the approximate frequency-domain channel equality between the method without IVI self-cancellation (corresponding to conventional differential) and the method with IVI self-cancellation (corresponding to two-hop differential).

V. CONCLUSION

A novel two-hop differential OSDM system is proposed in this paper to counteract the time-varying fading effect over UWA channels. It mainly provides two attractive features: 1) the implementation of differential detection obviates the necessity of channel estimation, leading to a substantial reduction of complexity at the receiver; 2) a two-hop differential scheme is designed for IVI self-cancellation, resulting in significant improvement of the system performance over time-varying UWA channels. The results suggest that, the two-hop differential OSDM system is easy to implement and thus holds promise for practical use.

REFERENCES

[1] A. Song, M. Stojanovic, and M. Chitre, "Editorial Underwater Acoustic Communications: Where We Stand and What Is Next?," *IEEE J. Ocean. Eng.*, vol. 44, no. 1, pp. 1-6, Jan. 2019.

[2] L. Liu, S. Zhou, and J.-H. Cui, "Prospects and problems of wireless communication for underwater sensor networks," *Wireless Commun. Mobile Comput.*, vol. 8, no. 8, pp. 977-994, Aug. 2008.

[3] M. Stojanovic, "Recent advances in high-speed underwater acoustic communications," *IEEE J. Ocean. Eng.*, vol. 21, no. 2, pp. 125-136, Apr. 1996.

[4] M. Stojanovic and J. Preisig, "Underwater acoustic communication channels: Propagation models and statistical characterization," *IEEE Commun. Mag.*, vol. 47, no. 1, pp. 84-89, Jan. 2009.

[5] Y. R. Zheng, C. Xiao, T. Yang, and W.-B. Yang, "Frequency-domain channel estimation and equalization for shallow-water acoustic communications," *J. Phys. Commun.*, vol. 3, no. 1, pp. 48-63, Mar. 2010.

[6] Z. Wang and G. B. Giannakis, "Wireless multicarrier communications: Where Fourier meets Shannon," *IEEE Signal Process. Mag.*, vol. 17, no. 3, pp. 29-48, May 2000.

[7] Y. Rahmatallah and S. Mohan, "Peak-to-average power ratio reduction in OFDM systems: A survey and taxonomy," *IEEE Commun. Surveys Tuts.*, vol. 15, no. 4, pp. 1567-1592, Oct. 2013.

[8] D. Falconer, S. Ariyavisitakul, A. Benyamin-Seeyar, and B. Eidson, "Frequency domain equalization for single-carrier broadband wireless systems," *IEEE Commun. Mag.*, vol. 40, no. 4, pp. 58-66, Apr. 2002.

[9] F. Pancaldi, G. Vitetta, R. Kalbasi, N. Al-Dhahir, M. Uysal, and H. Mheidat, "Single-carrier frequency domain equalization," *IEEE Commun. Mag.*, vol. 25, no. 5, pp. 37-56, Sep. 2008.

[10] N. Suehiro, C. Han, T. Imoto, and N. Kuroyanagi, "An information transmission method using Kronecker product," in *Proc. IASTED Int. Conf. Commun. Syst. Netw.*, Sep. 2002, pp. 206-209.

[11] X.-G. Xia, "Precoded and vector OFDM robust to channel spectral nulls and with reduced cyclic prefix length in single transmit antenna systems," *IEEE Trans. Commun.*, vol. 49, no. 8, pp. 1363-1374, Aug. 2001.

[12] T. Ebihara and K. Mizutani, "Underwater acoustic communication with an orthogonal signal division multiplexing scheme in doubly spread channels," *IEEE J. Ocean. Eng.*, vol. 39, no. 1, pp. 47-58, Jan. 2014.

[13] T. Ebihara and G. Leus, "Doppler-resilient orthogonal signal-division multiplexing for underwater acoustic communication," *IEEE J. Ocean. Eng.*, vol. 41, no. 2, pp. 408-427, Apr. 2016.

[14] J. Han, S. P. Chepuri, Q. Zhang, and G. Leus, "Iterative Per-Vector Equalization for Orthogonal Signal-Division Multiplexing Over Time-Varying Underwater Acoustic Channels," *IEEE J. Ocean. Eng.*, vol. 44, no. 1, pp. 240-255, Jan. 2019.

[15] J. Han, L. Zhang, Q. Zhang, and G. Leus, "Low-Complexity Equalization of Orthogonal Signal-Division Multiplexing in Doubly-Selective Channels," *IEEE Trans. Signal Process.*, vol. 67, no. 4, pp. 915-929, Feb. 2019.

[16] M. Stojanovic, "A method for differentially coherent detection of OFDM signals on Doppler-distorted channels," in *Proc. IEEE Sens. Array Multichannel Signal Process. Workshop*, Oct. 2010, pp. 85-88.

[17] B. M. Hochwald and W. Sweldens, "Differential unitary space-time modulation," *IEEE Trans. Commun.*, vol. 48, no. 12, pp. 2041-2052, Dec. 2000.

[18] B. L. Hughes, "Differential space-time modulation," *IEEE Trans. Inf. Theory*, vol. 46, no. 7, pp. 2567-2578, Nov. 2000.

[19] Y. Zhao and S. G. Haggman, "Intercarrier interference self-cancellation scheme for OFDM mobile communication systems," *IEEE Trans. Commun.*, vol. 49, no. 7, pp. 1185-1191, Jul. 2001.

[20] G. Leus and P. A. van Walree, "Multiband OFDM for Covert Acoustic Communications," *IEEE J. Select. Areas Commun.*, vol. 26, no. 9, pp. 1662-1673, Dec. 2008.

[21] Z. Liu and G. B. Giannakis, "Block differentially encoded OFDM with maximum multipath diversity," *IEEE Trans. Wireless Commun.*, vol. 2, no. 3, pp. 420-423, May 2003.

[22] J. Han, Y. Wang, Z. Gong, and G. Leus, "Equalization of OSDM over time-varying channels based on diagonal-block-banded matrix enhancement," *Signal Process.*, vol. 168, 107333, Mar. 2020.